Supporting Information

Trapped Ion Mobility Spectrometry, Ultraviolet Photodissociation and ToF Mass Spectrometry for Gas-Phase Peptide Isobars/Isomers/Conformers Discrimination

Samuel A. Miller,[†,#] Kevin Jeanne Dit Fouque,[†,‡,#] Mark E. Ridgeway,[§] Melvin A. Park,[§] and Francisco Fernandez-Lima.*[,†,‡]

[†] Department of Chemistry and Biochemistry, Florida International University, Miami, FL 33199, United States.

[‡] Biomolecular Sciences Institute, Florida International University, Miami, FL 33199, United States.

[§] Bruker Daltonics Inc., Billerica, MA 01821, United States.

[#] These authors contributed equally to this work.

Corresponding Author

fernandf@fiu.edu

Table of Contents:

Scheme S1. Simplified schematics of the nESI-TIMS-Trap UVPD section integrated into an existing Bruker Maxis Impact II ToF MS platform

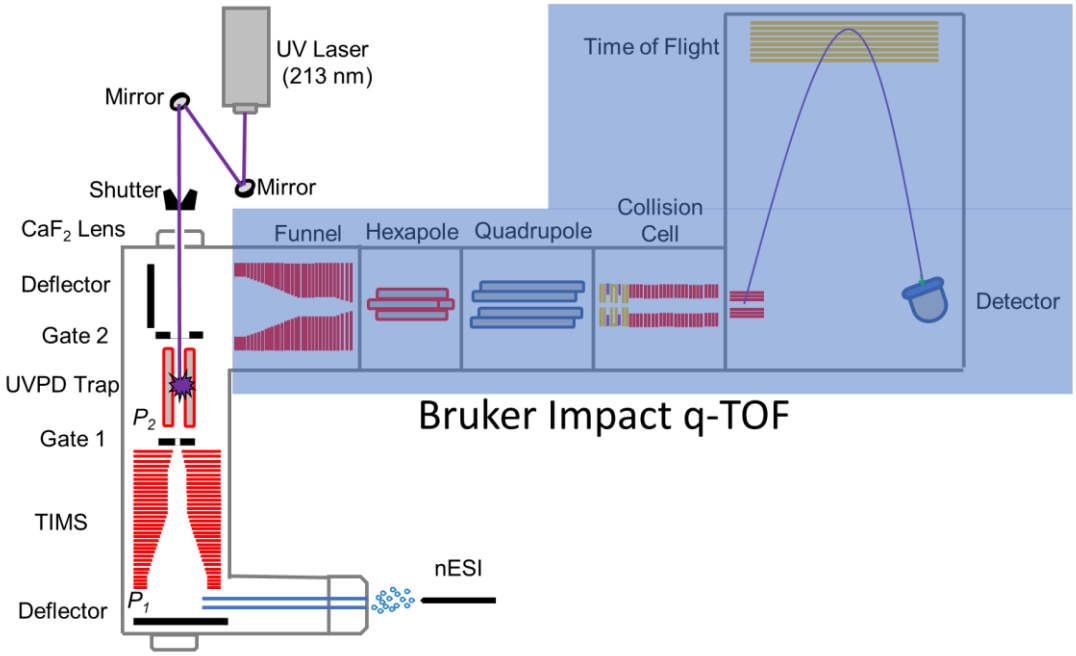

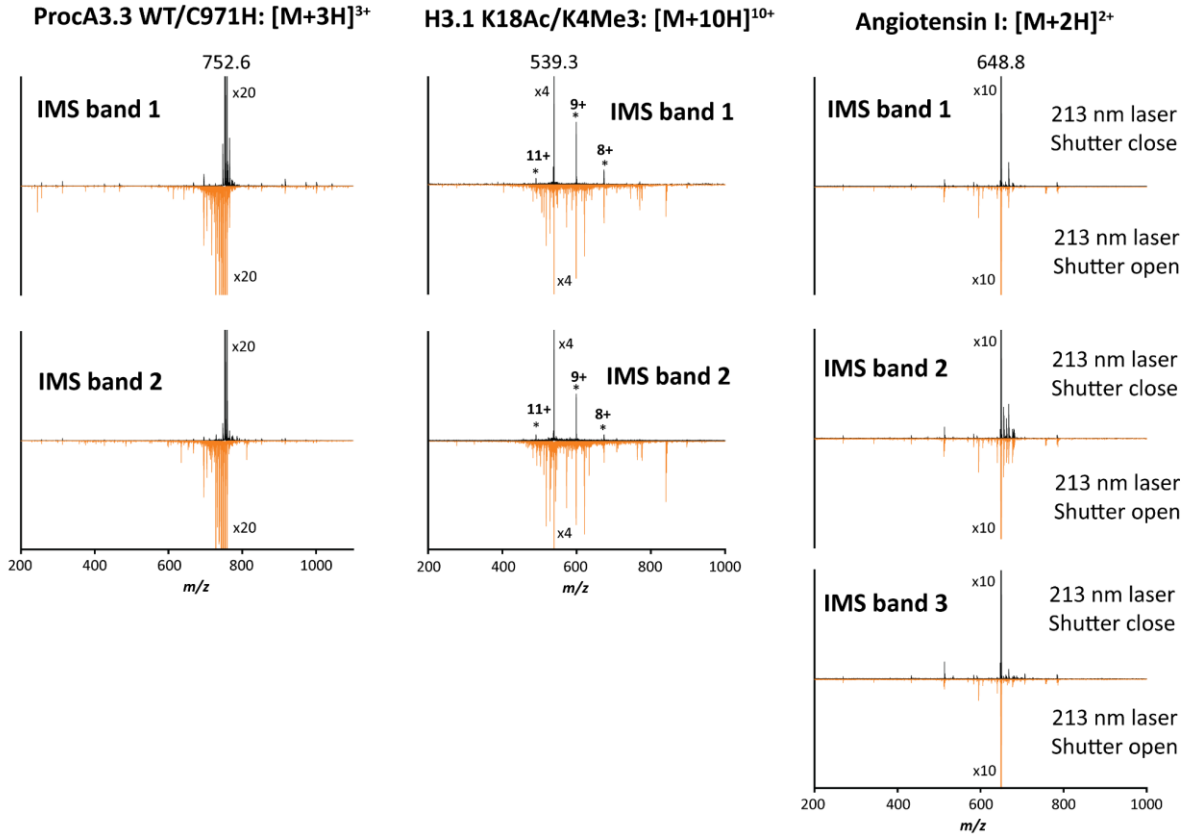

Figure S1. Comparison between IMS/MS spectra per ion mobility band when the 213 nm UV laser shutter is close (top) and open (bottom) for (a) ProcA3.3 regioisomers, (b) histone tails K18Ac/K4Me3 isobars and (c) angiotensin I conformers. Note that * symbols refer to other charge states contribution due to overlap in the mobility domain.

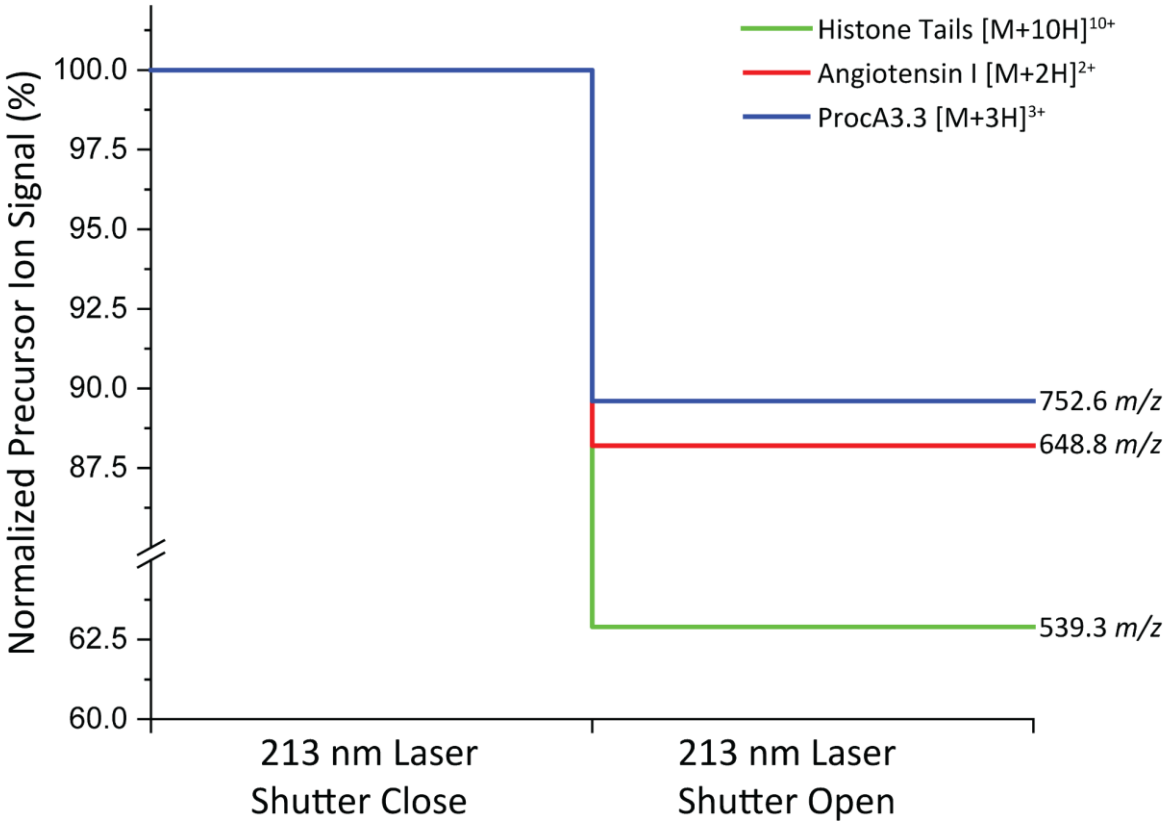

Figure S2. UVPD fragmentation efficiencies for all investigated peptides.

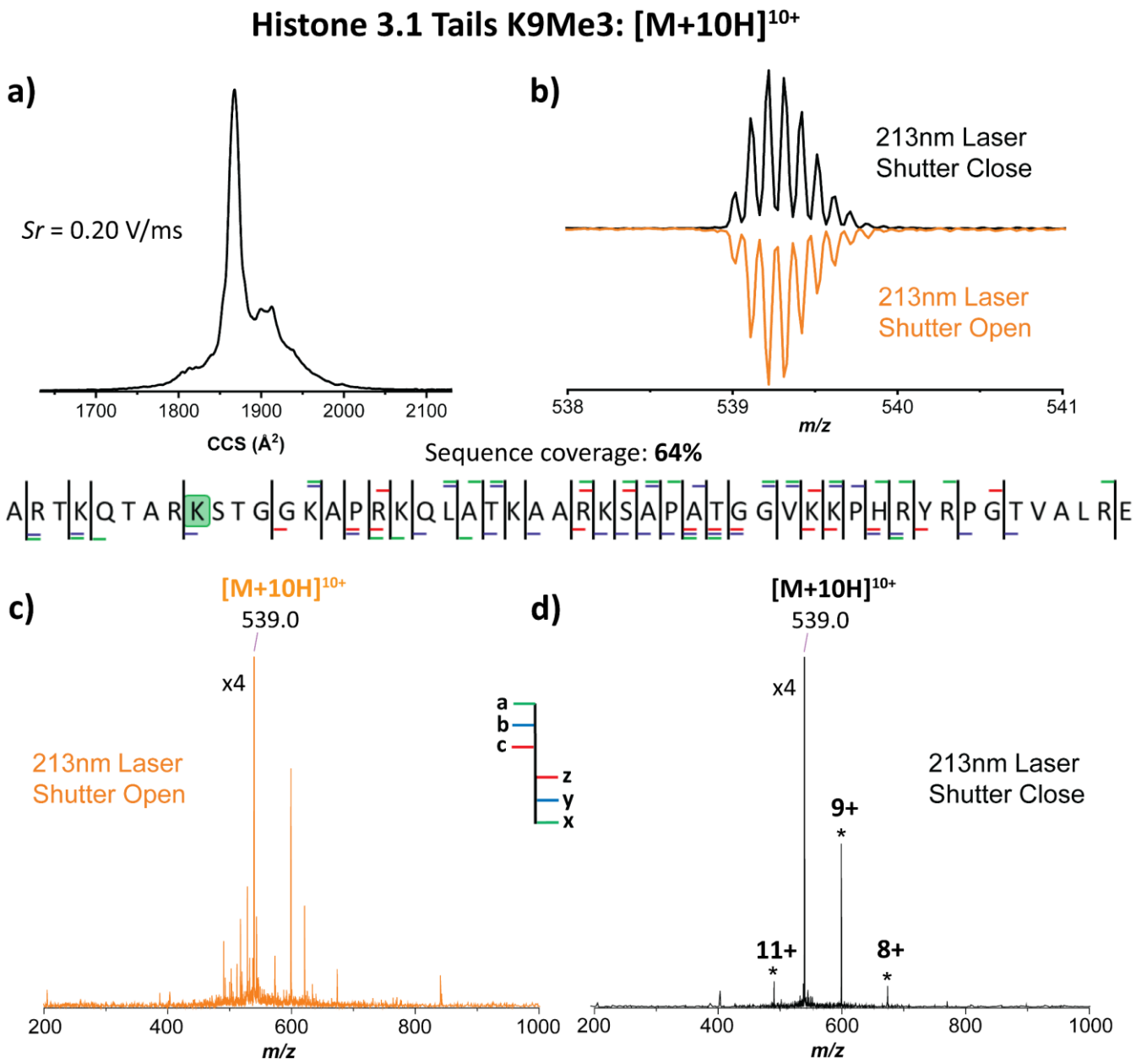

Figure S3. TIMS-UVPD-ToF MS analysis of the selected [M + 10H]$^{10+}$ species of K9Me3 (*m/z* 539.0). (a) TIMS profile, (b) isotopic pattern distribution of the precursor ion produced with UV laser shutter close (top) and with shutter open (bottom) and UVPD-IMS/MS spectra of the [M + 10H]$^{10+}$ species of K9Me3 when 213 nm laser shutter is (c) open (orange) and (d) close (black). Note that * symbols refer to other charge states contribution due to overlap in the mobility domain.

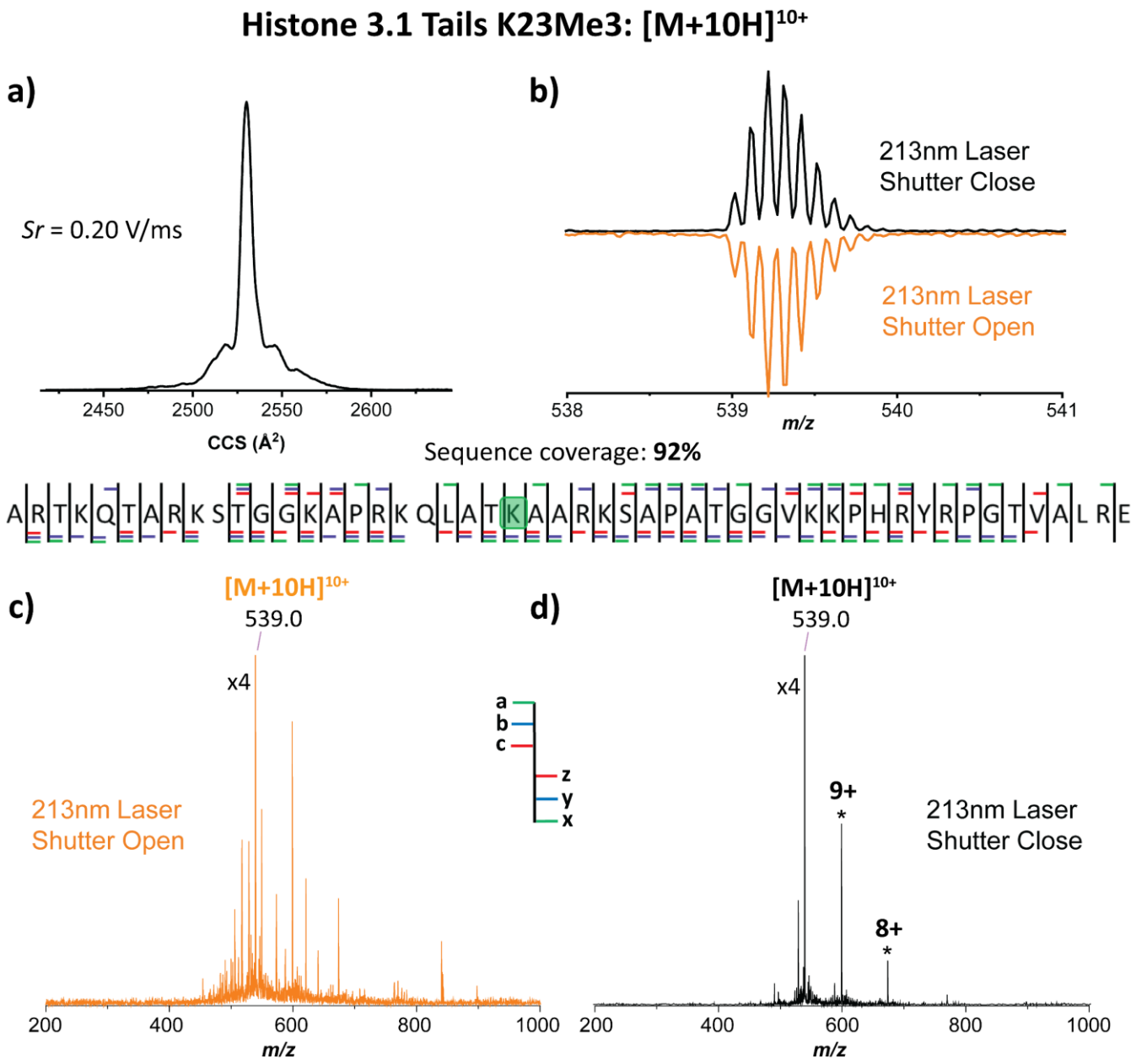

Figure S4. TIMS-UVPD-ToF MS analysis of the selected [M + 10H]$^{10+}$ species of K23Me3 (*m/z* 539.0). (a) TIMS profile, (b) isotopic pattern distribution of the precursor ion produced with UV laser shutter close (top) and with shutter open (bottom) and UVPD-IMS/MS spectra of the [M + 10H]$^{10+}$ species of K23Me3 when 213 nm laser shutter is (c) open (orange) and (d) close (black). Note that * symbols refer to other charge states contribution due to overlap in the mobility domain.

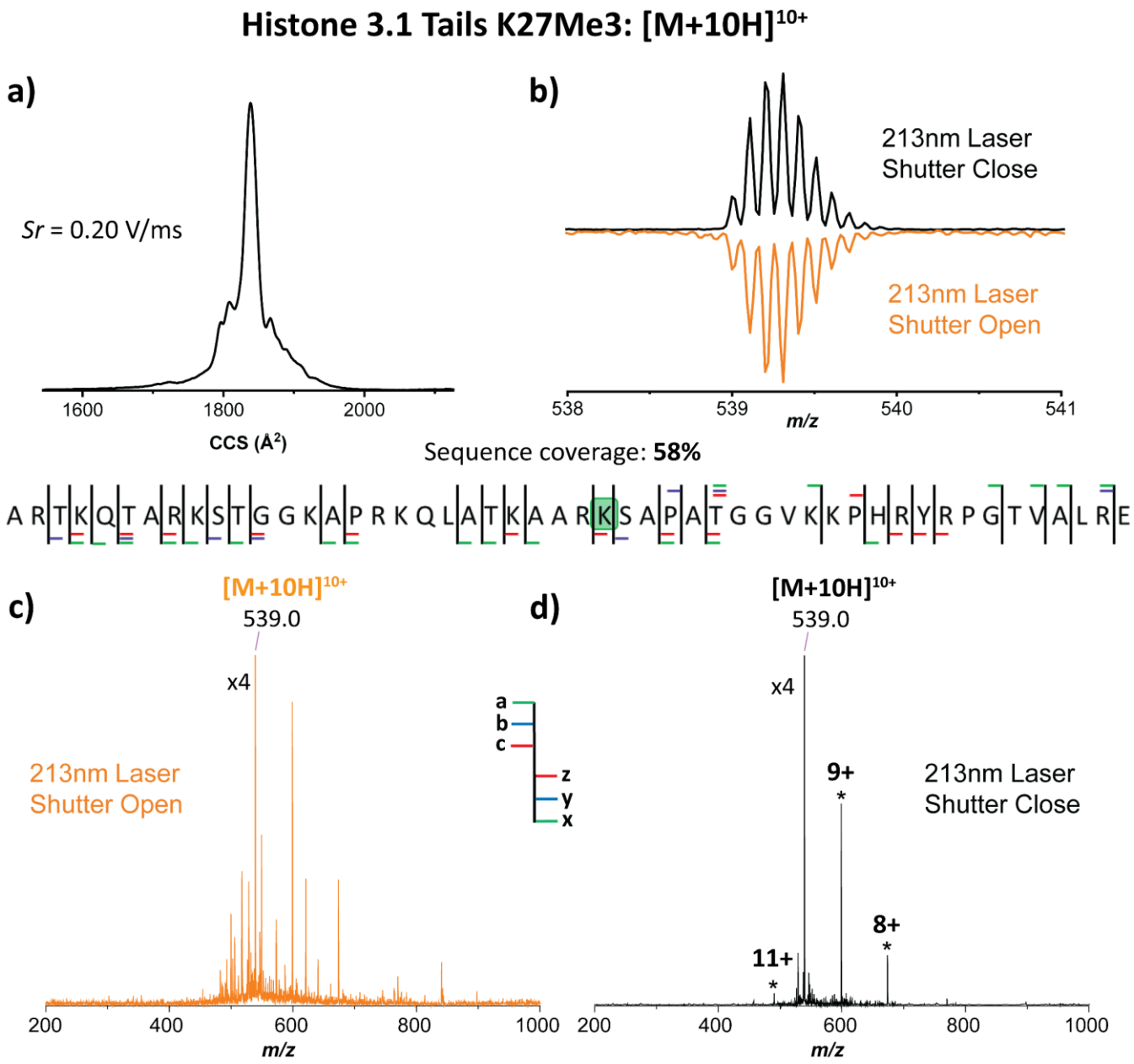

Figure S5. TIMS-UVPD-ToF MS analysis of the selected [M + 10H]$^{10+}$ species of K27Me3 (*m/z* 539.0). (a) TIMS profile, (b) isotopic pattern distribution of the precursor ion produced with UV laser shutter close (top) and with shutter open (bottom) and UVPD-IMS/MS spectra of the [M + 10H]$^{10+}$ species of K27Me3 when 213 nm laser shutter is (c) open (orange) and (d) close (black). Note that * symbols refer to other charge states contribution due to overlap in the mobility domain.

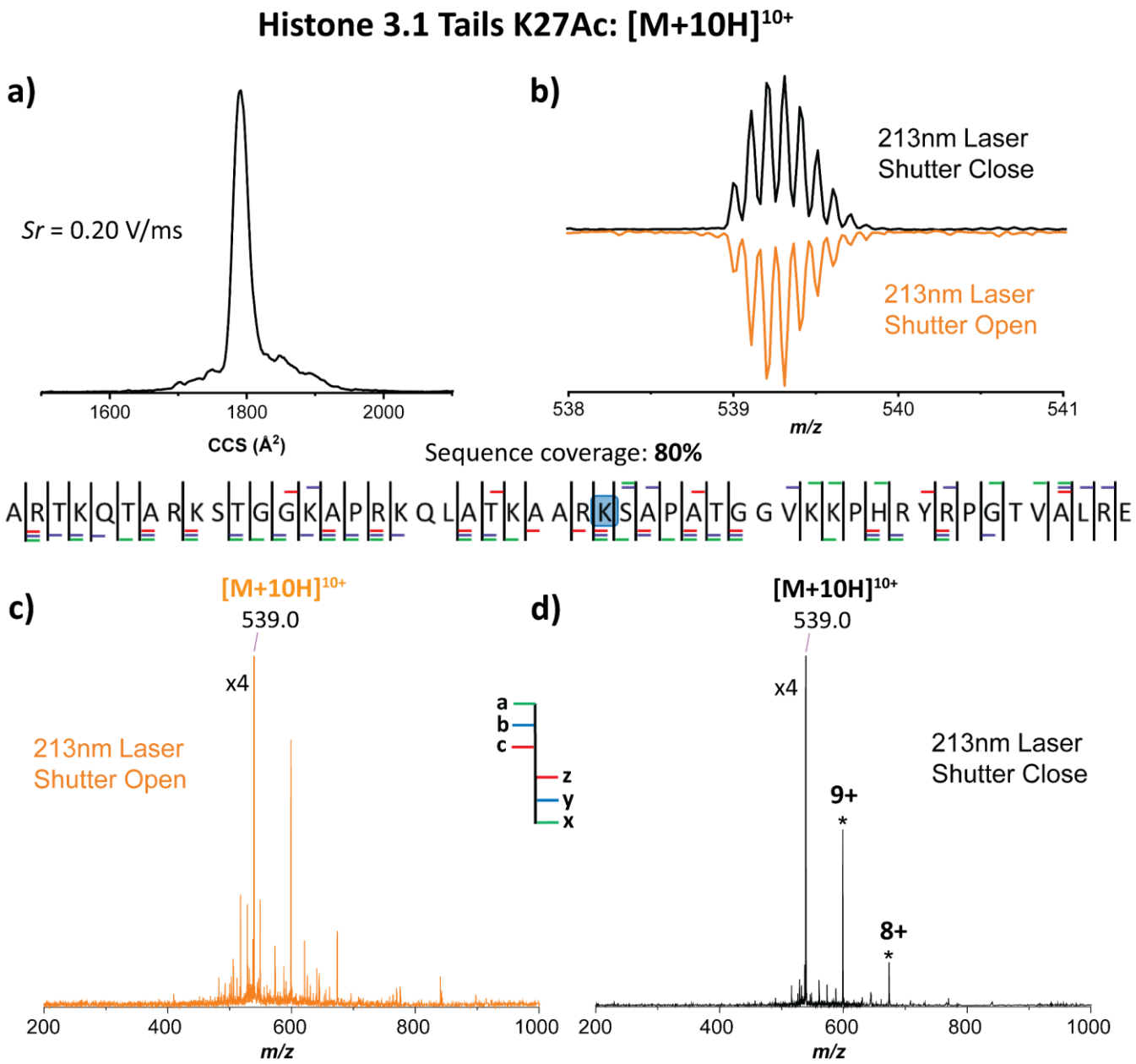

Figure S6. TIMS-UVPD-ToF MS analysis of the selected [M + 10H]$^{10+}$ species of K27Ac (*m/z* 539.0). (a) TIMS profile, (b) isotopic pattern distribution of the precursor ion produced with UV laser shutter close (top) and with shutter open (bottom) and UVPD-IMS/MS spectra of the [M + 10H]$^{10+}$ species of K27Ac when 213 nm laser shutter is (c) open (orange) and (d) close (black). Note that * symbols refer to other charge states contribution due to overlap in the mobility domain.

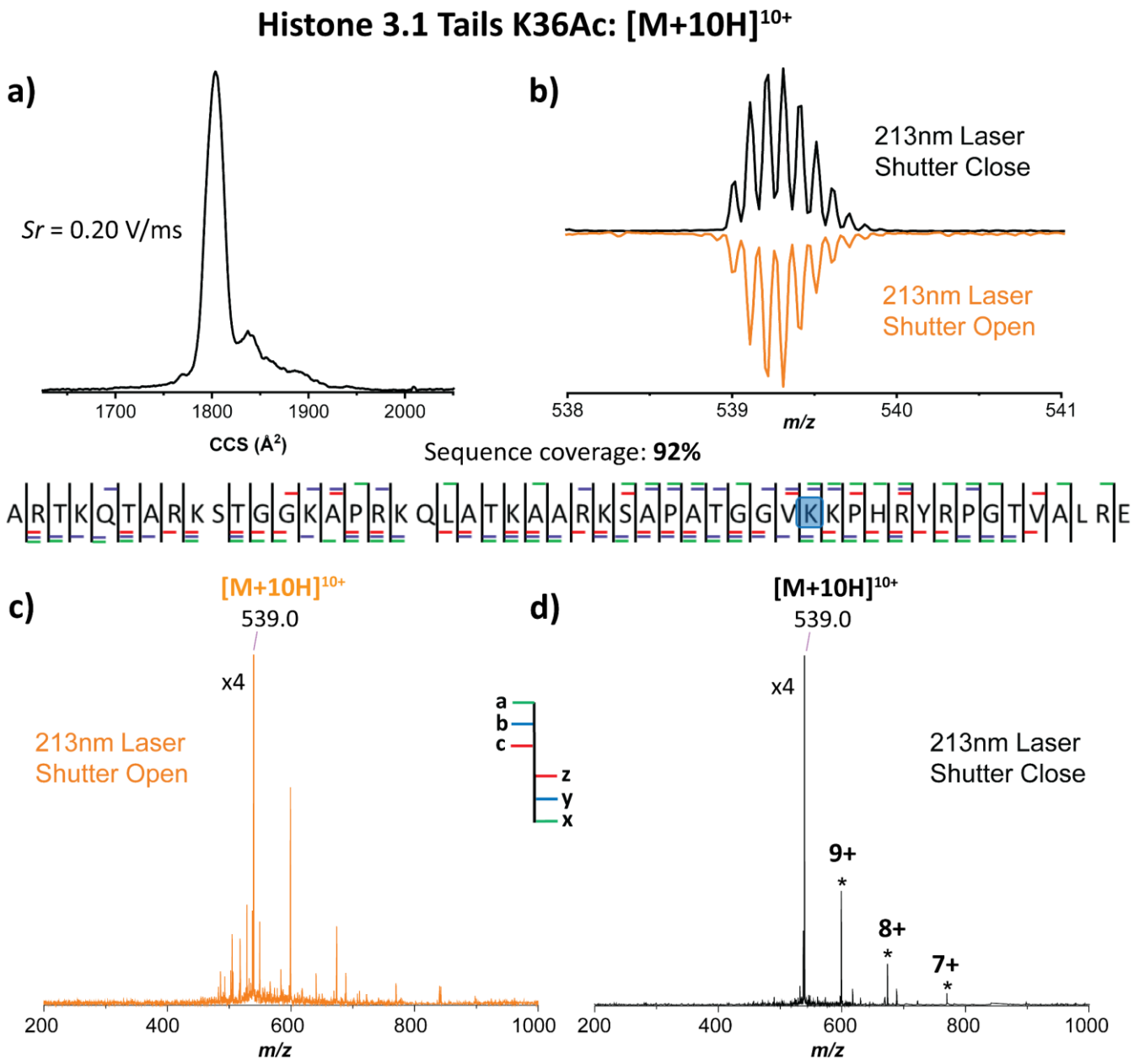

Figure S7. TIMS-UVPD-ToF MS analysis of the selected [M + 10H]$^{10+}$ species of K36Ac (*m/z* 539.0). (a) TIMS profile, (b) isotopic pattern distribution of the precursor ion produced with UV laser shutter close (top) and with shutter open (bottom) and UVPD-IMS/MS spectra of the [M + 10H]$^{10+}$ species of K36Ac when 213 nm laser shutter is (c) open (orange) and (d) close (black). Note that * symbols refer to other charge states contribution due to overlap in the mobility domain.

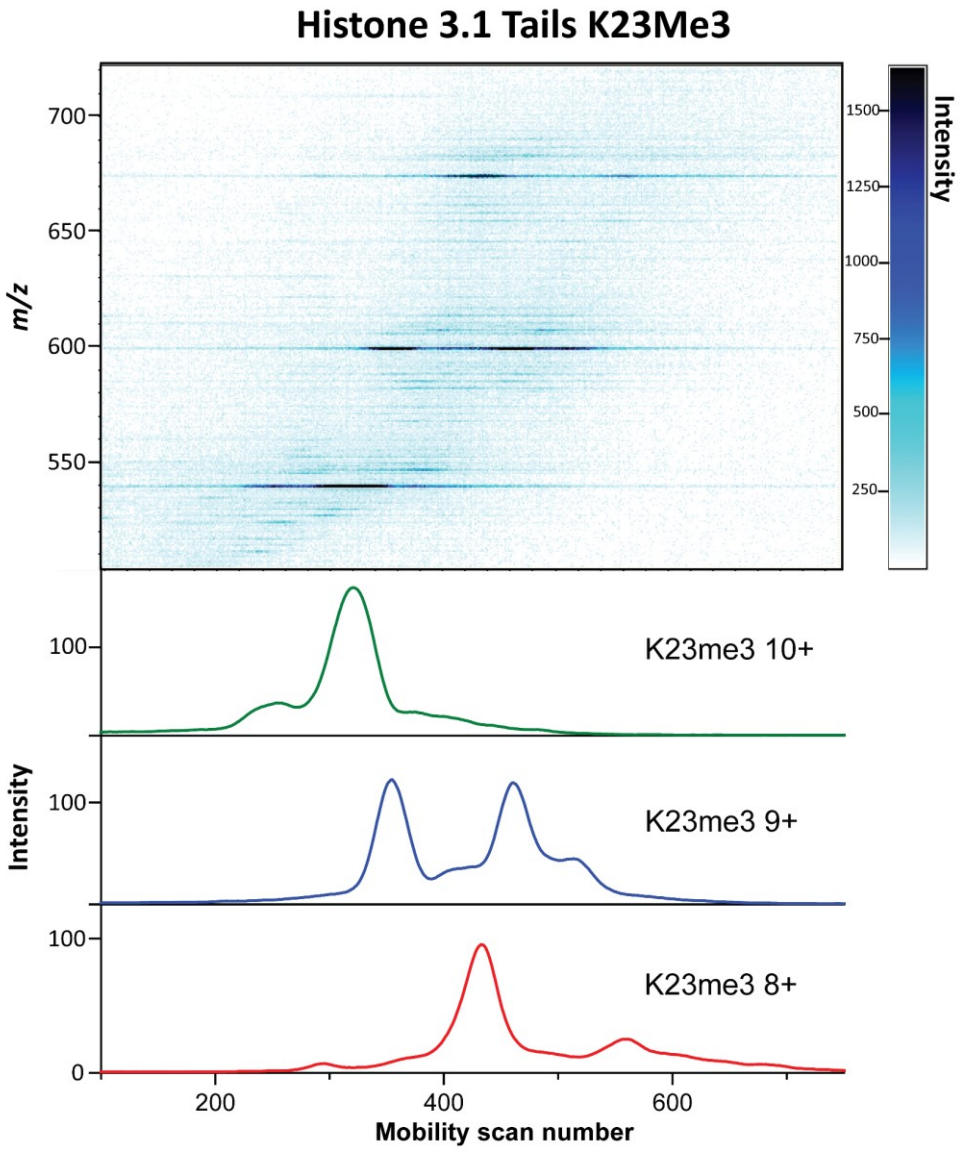

Figure S8. 2D-TIMS-MS contour map and extracted IMS spectra for the $[M + 8H]^{8+}$ (red), $[M + 9H]^{9+}$ (blue) and $[M + 10H]^{10+}$ (green) species of K23Me3.

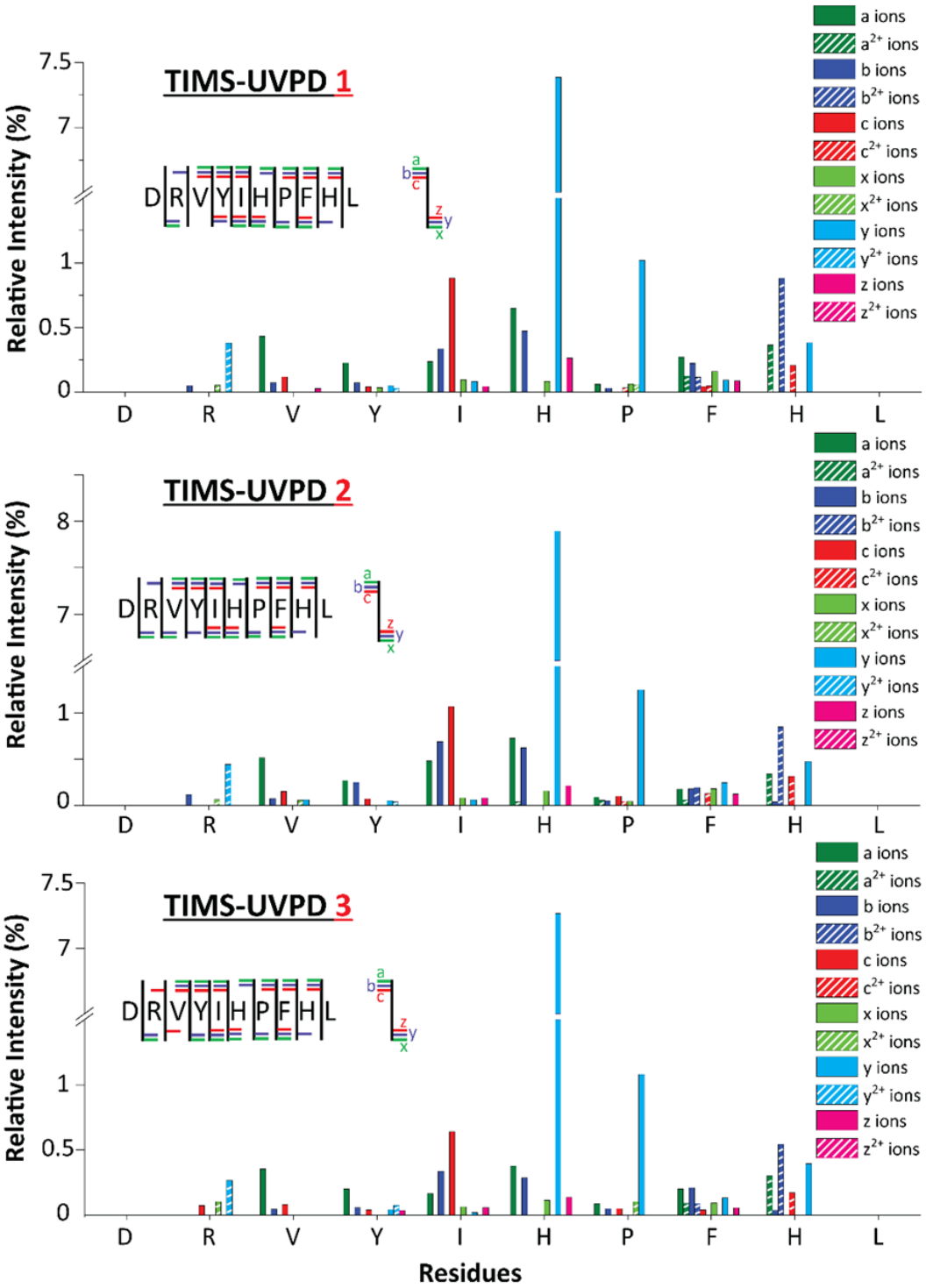

Figure S9. TIMS-UVPD-ToF MS analysis of the selected [M + 2H]2+ species of angiotensin I (m/z 648.9). Bar plots showing the relative intensities of the UVPD product ions per IMS bands. Note that relative intensities were calculated using peak heights and divided by the sum of all fragments for direct comparison across IMS bands.

Table S1. Relative intensities of the fragments per IMS band 1-3 of the TIMS-UVPD-ToF MS analysis of the selected [M + 2H]2+ species of angiotensin I (m/z 648.9).

Ratio of the relative intensities per IMS band 1-3			
IMS1/IMS2	IMS1/IMS3	IMS2/IMS3	Fragment
1	1	1	
0.87	0.61	0.70	a_2
0.84	1.22	1.45	a_3
0.83	1.11	1.35	a_4
0.49	1.42	2.89	a_5
0.89	1.34	1.51	a_6
0.36	0.42	1.17	a_6^{2+}
0.67	0.70	1.04	a_7
0.42	1.21	2.89	a_7^{2+}
1.53	1.35	0.88	a_8
1.91	1.34	0.70	a_8^{2+}
1.06	1.20	1.13	a_9^{2+}
0.44	3.57	8.18	b_2
0.97	1.62	1.66	b_3
0.29	1.23	4.26	b_4
0.49	1.00	2.05	b_5
0.76	1.29	1.70	b_6
0.52	1.35	2.61	b_6^{2+}
0.61	0.61	1.00	b_7
0.71	0.75	1.07	b_7^{2+}
1.25	1.06	0.85	b_8
0.59	1.27	2.15	b_8^{2+}
0.29	0.31	1.07	b_9
1.04	1.61	1.56	b_9^{2+}
0.19	0.10	0.52	c_2
0.76	1.43	1.88	c_3
0.58	1.03	1.77	c_4
0.83	1.38	1.67	c_5
0.20	0.40	1.97	c_7

0.76	1.04	1.37	c_7^{2+}
2.31	1.07	0.46	c_8
0.37	1.69	4.56	c_8^{2+}
0.66	1.20	1.82	c_9^{2+}
0.88	1.71	1.94	x_3
1.37	5.64	4.12	x_4
0.89	0.55	0.62	x_4^{2+}
0.52	0.72	1.38	x_5
1.13	1.48	1.30	x_6
1.07	0.66	0.62	x_6^{2+}
0.92	1.25	1.35	x_7
0.19	0.37	1.92	x_8^{2+}
0.82	0.52	0.64	x_9^{2+}
0.80	0.96	1.20	y_2
0.38	0.70	1.85	y_3
0.82	0.94	1.16	y_4
0.85	0.32	0.38	y_4^{2+}
0.94	1.02	1.09	y_5
1.34	3.88	2.90	y_6
0.95	1.14	1.20	y_7
0.75	0.40	0.53	y_7^{2+}
0.42	1.07	2.54	y_8
0.85	1.42	1.66	y_9^{2+}
0.69	1.50	2.18	z_3
1.23	1.91	1.56	z_5
0.53	0.77	1.44	z_6
0.29	0.13	0.44	z_7
1.27	1.26	0.99	z_8